Journal of Biomedical Materials Research Part B: Applied Biomaterials

WILEY

Society For Biomaterials

TECHNICAL NOTE OPEN ACCESS

Targeted Delivery of Microneurotrophin BNN27 via Biomaterial Grafts Protects Retinal Ganglion Cells After Optic Nerve Injury

K. Georgelou[1,2] | E. A. Saridaki[2] | C. P. Apostolidou[3,4] | X. Mallios[2] | A. Papagiannaki[1] | K. Karali[1,2] | T. Katsila[5] | T. Calogeropoulou[5] | A. Mitraki[3,4] | D. Karagogeos[1,6] | I. Charalampopoulos[1,2] | A. Gravanis[1,2] | M. Savvaki[1,6] | D. S. Tzeranis[1,3,7]

[1]Institute of Molecular Biology and Biotechnology, Foundation for Research and Technology – Hellas, Heraklion, Greece | [2]Department of Pharmacology, School of Medicine, University of Crete, Heraklion, Greece | [3]Department of Materials Science and Engineering, University of Crete, Heraklion, Greece | [4]Institute of Electronic Structure and Laser, Foundation for Research and Technology – Hellas, Heraklion, Greece | [5]Institute of Chemical Biology, National Hellenic Research Foundation, Athens, Greece | [6]Department of Basic Science, School of Medicine, University of Crete, Heraklion, Greece | [7]Department of Mechanical and Manufacturing Engineering, University of Cyprus, Nicosia, Cyprus

Correspondence: D. S. Tzeranis (dtzeranis@uoc.gr)

Received: 28 July 2025 | **Revised:** 14 November 2025 | **Accepted:** 8 December 2025

Keywords: biomaterial grafts | microneurotrophins | neuroprotection | optic nerve injury | targeted delivery

ABSTRACT

Emerging neurotrophin treatments for optic nerve injury (ONI) aim to prevent the loss of retinal ganglion cells (RGCs) and enhance axonal regeneration. Microneurotrophins (MNTs), small-molecule mimetics of neurotrophins, have shown neuroprotective effects in various animal models of neurodegeneration, yet MNT effects on ONI remain unknown. Here, we study the effects of BNN27, a MNT that mimics NGF, in a mouse model of optic nerve crush (ONC) and compare the targeted administration via biomaterial grafts placed around the ONC lesion against standard eye drop delivery. Compared to eye drop delivery, targeted biomaterial-based BNN27 delivery resulted in more consistent and efficient RGC neuroprotection and reduced microglia-mediated inflammation in the ONC lesion. Our findings demonstrate that targeted delivery of MNTs can alleviate key consequences of ONI and, therefore, be an essential part of effective combinatorial ONI treatments.

1 | Introduction

Optic nerve injury (ONI) leads to irreversible vision loss due to retinal ganglion cell (RGC) death and the inability of axon regeneration. Currently, there are no effective treatments for ONI [1–3]. Various therapeutic strategies, including BAX inhibition, PTEN knockdown, and cAMP administration, have been evaluated in animal models [4, 5], but are limited by unfavorable pharmacokinetics [6] or by the complexities of genetic manipulations [7].

Research has focused on ONI treatments based on neurotrophins (NTs; NGF, BDNF, NT3, NT4/5) as NTs are implicated in neuronal survival, axonal outgrowth, and synaptic plasticity [8, 9]. In the retina, NTs are both produced locally and retrogradely transported via RGC axons [10]. According to the NT hypothesis, ONI stops retrograde transport via the optic nerve and results in the deprivation of NT support to RGCs, leading to apoptotic cell death [11]. Thus, NT treatments aim to prevent RGC loss and enhance RGC axon elongation. Indeed, ocular administration of NGF reduced RGC loss following ONI [12–14]. However, NT treatments are limited by poor pharmacokinetics and side effects [15, 16].

To address these issues, various small-molecule NT mimetics have been developed, including microneurotrophins (MNTs),

lipophilic C17-spirocyclic derivatives of dehydroepiandrosterone (DHEA) that can selectively activate neurotrophin receptors (NTRs) and pass the brain–blood barrier [17, 18]. BNN27, the seminal MNT, is an NGF mimetic that can activate both NGF receptors (TrkA, $p75^{NTR}$). Previous pharmacokinetic studies have demonstrated the presence of BNN27 in rodent brain and retina 30 min after intraperitoneal (i.p.) injection. BNN27 concentration peaked in the retina 2 h after i.p. injection and could not be detected 4 h later [19, 20]. BNN27 has demonstrated neuroprotective effects on various kinds of neurons in vitro, which were mediated via both NGF receptors and downstream pro-survival pathways [21, 22]. BNN27 administration decreased retina cell apoptosis in a rat model of diabetes-induced retinal damage via TrkA activation and $p75^{NTR}$ downregulation [23, 24]. BNN27 demonstrated effects on glial cells (oligodendrocytes rescue, reduction of astrogliosis and microgliosis) in a mouse cuprizone-induced model of demyelination [25]. Finally, systemic administration of BNN27 in the mouse dorsal column crush spinal cord injury (SCI), reduced astrogliosis, and increased neuron density in the SCI lesion at 12 weeks post-injury (wpi) [26].

The present study evaluates the effects of BNN27 in a mouse model of optic nerve crush (ONC), an established animal ONI model of clinical relevance. Motivated by the retrograde mechanism of NT support of RGCs, we developed a biomaterial-based system for the targeted delivery of BNN27 directly on the optic nerve. The system consisted of a BNN27-loaded N-(fluorenylmethyloxycarbonyl)-Phenylalanine-Phenylalanine (Fmoc-Phe-Phe, hereinafter referred to as "FmocFF," Figure 2d) peptide hydrogel formed inside a porous collagen-glycosaminoglycan (GAG) scaffold (CGS). FmocFF hydrogels were pioneered by the Gazit group as minimal, self-assembling peptide hydrogels able to encapsulate and deliver model compounds in a controlled manner [27]. The Fmoc group is an N-terminal protecting group used in solid phase peptide synthesis, which induces self-assembly of peptide building blocks into supramolecular structures (such as tubes, fibrils, hydrogels) mainly driven by π-π* aromatic stacking interactions. Fmoc-based hydrogels are attractive candidates for biomedical applications (reviewed in [28]). FmocFF hydrogels have been extensively used for drug delivery applications [29], including NSAIDs [30], photosensitizers with antibacterial [31] and wound healing properties [32], and anticancer drugs [33–35]. In this work, the hydrogel was formed via the "solvent switch" method that involves dissolving the peptide building blocks in a solubilizing "good" solvent followed by the addition of a "bad" solvent that initiates peptide self-assembly and gelation [27]. Our results show that BNN27 administration (via eye drops or CGS-FmocFF grafts) significantly enhanced RGC survival at 2 wpi. BNN27 delivery via grafts provided more consistent and efficient neuroprotection compared to delivery via eye drops. In addition, only BNN27 delivery via graft delivery significantly reduced microglia-mediated inflammation in the ONC site. Although BNN27 failed to induce significant RGC axonal elongation at 2 wpi, the neuroprotective effects of BNN27 suggest that targeted biomaterial-based delivery of MNTs can be an essential part of effective combinatorial ONI treatments.

2 | Methods

2.1 | Animals

Animal experiments took place in the IMBB-FORTH animal facility (license number EL91-BIOexp-02). Animal care and experimentation protocols were performed according to the Veterinary Directorate of the Region of Crete in compliance with Greek Government guidelines, EU guidelines 2010/63/EU, FORTH ethics committee guidelines in accordance with approved protocols from the Federation of European Laboratory Animal Science Associations (FELASA) (approval numbers: 262272 and 360667, date of initial approval: October 29, 2018. Date of reapproval: November 29, 2021). C57/BL6 mice (The Jackson Laboratory) were maintained in climate-controlled conditions (30%–50% humidity, 21°C ± 2°C temperature, 12:12 h light/dark cycle) with ad libitum access to food and water.

2.2 | CGS-FmocFF Graft Fabrication

Porous CGS sheets were fabricated by lyophilizing a 5 mg/mL microfibrillar collagen I suspension in 50 mM acetic acid including 0.44 mg/mL chondroitin-6-sulfate [36]. The resulting dry sheets (2.5 mm thick, 0.5% mass fraction, 95 μm mean pore diameter) were cross-linked via dehydro-thermal treatment (105°C, 50 mTorr, 24 h); 4 × 3 × 1.5 mm CGS pieces were cut from sheets. CGS structure was verified by scanning electron microscopy (SEM).

BNN27-loaded CGS-FmocFF grafts were prepared by soaking a 4 × 3 × 1.5 mm CGS piece with 6 μL BNN27-FmocFF peptide solution (7.5 mM BNN27 2 mg/mL FmocFF in 25% (v/v) ethanol) immediately after mixing 2 μL FmocFF-BNN27 stock solution (30 mM BNN27 8 mg/mL FmocFF in ethanol) with 6 μL dH_2O. In this case ethanol acts as the "good" solvent for FmocFF peptides, while water acts as the "bad" solvent that triggers self-assembly and gelation of FmocFF peptides that entraps BNN27. Within seconds the solution enters CGS pores (via sponge action), where FmocFF peptides self-assemble and form a hydrogel that encapsulates BNN27. FmocFF hydrogel structure was verified by SEM.

2.3 | Quantification of BNN27 Delivery Kinetics In Vitro

2 μL of FmocFF–BNN27 stock solution [2 mg FmocFF (Bachem #4015688) and 2.5 mg BNN27 in 250 μL ethanol] was mixed with 6 μL dH_2O resulting in 7.5 mM BNN27 2 mg/mL FmocFF solution in 25% (v/v) ethanol. Upon mixing, the solution was incubated for 5 min at room temperature to induce the formation of a FmocFF hydrogel, which was then submersed in 50 μL release buffer (0.05% Tween20 in PBS) and incubated at 37°C. At specific time points (t_i = 3, 6, 24, 72, 120 h following hydrogel preparation), V_s = 50 μL solution was removed and replaced with V_s μL fresh release buffer. The concentration C_i of BNN27 in the solutions sampled at t_i was measured using

a cholesterol assay kit (Biosis #001977) per manufacturer instructions. The amount n_i of BNN27 that was released up to t_i was calculated from C_i using the formula $n_i = V_s \cdot \left(\sum_{j=1}^{i} C_j\right)$.

The resulting release response $n_i = n(t_i)$ was then used to fit an exponential function

$$n(t) = n_{\text{tot}}\left(1 - e^{-t/\tau}\right)$$

where τ is the release time constant and n_{tot} is the total amount of BNN27 that can be released by a FmocFF hydrogel (nominally $n_0 = 60$ nmol). The release experiment was repeated three times.

2.4 | ONC Model

This study adapted a standard mouse ONC model [37, 38] to evaluate the effects of BNN27 delivered via eye drops or CGS-FmocFF grafts. All surfaces, tools, and instruments utilized had been sterilized carefully. Two-month-old C57/BL6 male mice underwent systemic anesthesia via i.p. injection of ketamine/xylazine. After verifying the absence of paw reflexes, each mouse was transferred onto a heat pad, where ophthalmic ointment was applied to the non-operated right eye to avoid eye dryness. Then, the conjunctiva of the left eye was incised, and the optic nerve was exposed at its exit from the eye globe by gently putting aside the orbital muscles. The optic nerve of the left eye was crushed approximately 1 mm away from the eyeball using a pair of Dumont #5 fine forceps for 10 s. Great care was taken not to damage the ophthalmic artery.

The study included six mice groups. In three groups, injured eyes were treated with 5 μL BNN27 eye drops (50 mM BNN27 in DMSO) applied once every 2nd day ["Crush+BNN27 (1 drop/2nd day)" group], once daily ["Crush+BNN27 (1 drop/day)" group], or twice daily ["Crush+BNN27 (2 drops/day)" group]. In the "Crush" group, injured eyes received 5 μL DMSO drops twice daily. All drop treatments started 1 day after ONC. In the "Crush+BNN27 (Graft)" group, a BNN27-loaded CGS-FmocFF graft was placed around the crushed optic nerve site immediately after ONC. In the "Crush (Graft)" group, a CGS-FmocFF graft was placed around the crushed optic nerve site immediately after ONC. Non-operated right eyes ("Intact" group) received the same BNN27 drop treatment as the corresponding injured left eye (no treatment when BNN27 was delivered via a graft). Mice were provided with meloxicam (Metacam) the day of operation and the following day for analgesia.

2.5 | Eye Tissue Collection, Preparation, and Quantification of BNN27

Mice were sacrificed at 1 or 2 wpi. Eyes were enucleated, fixed in 4% paraformaldehyde overnight, cryopreserved in 30% sucrose solution in 0.1 M phosphate buffer (PB) at 4°C for 24 h, placed in OCT embedding matrix (VWR #361603E), and snap frozen by immersion in isopentane cooled at −70°C. Eye bulbs and optic nerves were cryo-sectioned in 20 μm-thick cross sections and 10 μm-thick longitudinal sections, respectively. The presence of BNN27 in lysates of harvested tissues (retina, optic nerve) was quantified (detection limit 0.7 ng/mL) via liquid chromatography–mass spectrometry (LC-MSn) as previously described [39].

2.6 | Immunohistochemistry, Imaging, and Image Processing

Eye tissue (retina, optic nerve) sections on slides were placed in ice-cold acetone for 5 min, air-dried for 10 min in laminar flow, washed twice in PBS, once in 0.1% PBST and once in 0.3% PBST, blocked in 0.1% PBST supplemented with 0.1% BSA and 10% goat or horse serum at room temperature for 1 h, incubated in primary antibodies [Iba1: 1:1000 Wako #019-19741; L1: 1:000 (obtained by Dr. Fritz G. Rathjen); MAG: 1:200 Cell Signaling #9043; NeuN: 1:200 Millipore #MAB377; NF: 1:200 Biolegend #837904; $p75^{NTR}$: 1:100 Promega #G3231; TrkA: 1:100 Millipore #06-574] diluted in blocking solution at 4°C overnight, washed three times in 0.1% PBST, incubated with fluorophore-conjugated secondary antibodies (Thermo) diluted in PBS at room temperature for 1 h, washed once in 0.1% PBST and once in PBS, counterstained with Hoechst33342, washed once in PBS and once in PB, and mounted. For TrkA and TrkB immunohistochemistry, sections were incubated in preheated (85°C) 10 mM sodium citrate in PBS pH = 6.0 for 10 min, cooled down at room temperature, and washed in 0.1% PBST before blocking. Immunostained sections were imaged using a Leica TCS SP8 confocal microscope using 40× or 63× oil-immersion objective lens. Retina images were acquired (3–4 images per section) from peripheral retina cross sections. The quantification of $NeuN^+$ cells in peripheral ganglion cell layer (GCL) was expressed as linear density ($NeuN^+$ cells per 100 μm GCL length). Notably, unlike the central retina, the morphology of peripheral retina consists of a monolayer GCL, allowing the calculation of linear density. NTR expression was quantified by calculating the fraction of $p75^{NTR+}$ and $TrkA^+$ pixels within the GCL (GCL boundaries were defined manually). Images of optic nerve longitudinal sections were acquired at the injury site and distal to it (toward the optic chiasm). Axonal elongation was quantified by counting the number of $L1^+$ axons at various distances (250 μm, 500 μm, 750 μm, 1000 μm) from the proximal end of the injury site and results were expressed as linear density (axons per 100 μm of optic nerve). Microglia-mediated inflammation was quantified by counting the fraction of $Iba1^+$ pixels within the injury site. Image analysis tasks were performed in the Fiji software, with consistent thresholds to avoid background noise.

2.7 | Statistical Analysis

Experimental data are expressed as mean ± standard error of the mean (SEM). Statistical analysis was performed using the Prism software (GraphPad, La Jolla, USA). Statistical significance was assessed by unpaired two-tailed Student's *t*-tests (two-group comparisons) or one-way ANOVA followed by Tukey's post hoc test (multi-group comparisons). Statistical significance level was assumed at 0.05.

3 | Results

3.1 | Expression of NGF Receptors Following ONC

BNN27 has been shown to bind and activate the $p75^{NTR}$ and TrkA NTRs. Accordingly, we quantified the expression of $p75^{NTR}$ and TrkA in the GCL of peripheral retina at 2 wpi. Immunostaining was performed on the retina cross sections for $p75^{NTR}$ or TrkA, and the fraction of GCL pixels that stained positively for each marker was calculated (Figure 1a–c). Results showed that both $p75^{NTR}$ and TrkA were expressed in GCL cells. Small ONC-induced NTR expression alterations observed at 2 wpi ($p75^{NTR}$ upregulation, TrkA downregulation) were not statistically significant.

3.2 | Effects of BNN27 Delivered via Eye Drops Following ONC

Initially, we evaluated the effects of BNN27 delivered via eye drops in the mouse ONC model. To address the low bioavailability of eye drops for retinal delivery and the poor water solubility of BNN27 [19], we administered 5 μL DMSO eye drops containing the maximum possible concentration (50 mM) of BNN27. To determine the appropriate frequency of drop administration and evaluate the toxicity of eye drops, RGC survival was evaluated after a 2-week administration of four drop treatments in intact eyes: (a) no drops, (b) two DMSO drops daily, (c) one 50 mM BNN27 drop in DMSO daily, and (d) two 50 mM BNN27 drops in DMSO daily. As illustrated in Figure 1e, administration of

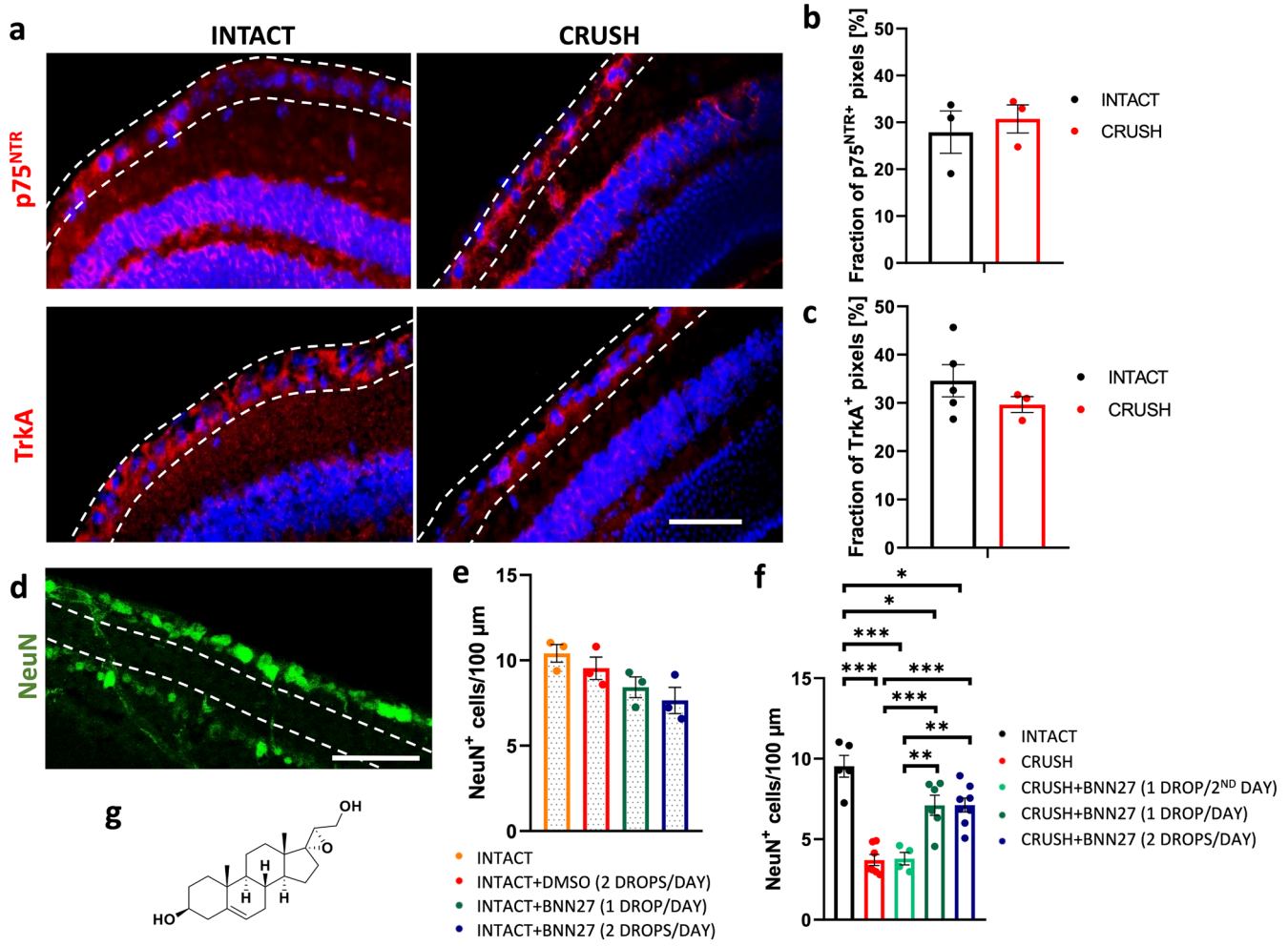

FIGURE 1 | Expression of NGF receptors in GCL and evaluation of BNN27 effects on RGC survival at 2 wpi when delivered via eye drops. (a) Representative fluorescence images of peripheral retina cross sections from intact and injured eyes at 2 wpi immunostained for $p75^{NTR}$ and TrkA (red). (b and c) Quantification of the fraction of $p75^{NTR+}$ and $TrkA^+$ pixels in the GCL of intact and injured eyes at 2 wpi ("Intact": $N = 3–5$; "Crush": $N = 3$). (d) Representative fluorescence image of an uninjured peripheral retina cross section immunostained for NeuN. (e) Quantification of $NeuN^+$ cell linear density in the GCL of four intact eye groups at 2 wpi ($n = 3$). (f) Quantification of $NeuN^+$ cell linear density in the GCL of intact and injured eye groups at 2 wpi ["Intact": $N = 5$; "Crush": $N = 7$; "Crush+BNN27 (1 drop/2nd day)": $N = 4$; "Crush+BNN27 (1 drop/day)": $N = 6$; "Crush+BNN27 (2 drops/day)": $N = 8$]. (g) Structure of BNN27. Results are presented as mean ± SEM. $^*p < 0.05$, $^{**}p < 0.01$, $^{***}p < 0.001$; Tukey's post hoc pairwise test assuming $p_{1\text{-way-ANOVA}} < 0.05$. Dotted lines denote GCL boundaries. Scale bars: 50 μm.

DMSO drops (with or without BNN27) did not result in a statistically significant reduction in NeuN$^+$ cell linear density in the GCL of the peripheral retina ["Intact": 10.4 ± 0.5 cells/100 μm; "Intact+DMSO (2 drops/day)": 9.7 ± 0.9 cells/100 μm, $p = 0.78$; "Intact+BNN27 (1 drop/day)": 8.4 ± 0.6 cells/100 μm, $p = 0.21$; "Intact+BNN27 (2 drops/day)": 7.6 ± 0.8 cells/100 μm, $p = 0.06$, $n = 3$].

Quantification of NeuN$^+$ cells in the GCL of peripheral retina showed that ONC induces a significant loss of RGCs at 2 wpi ("Intact": 9.5 ± 0.7 cells/100 μm, $n = 5$; "Crush": 3.6 ± 0.3 cells/100 μm, $n = 7$, $p < 10^{-4}$). Administration of one BNN27 drop per second day did not affect NeuN$^+$ cell density (3.8 ± 0.4 cells/100 μm, $n = 4$, $p > 0.99$). In contrast, daily administration of one or two BNN27 drops resulted in efficient neuroprotection ["Crush+BNN27 (1 drop/day)": 7.1 ± 0.6 cells/100 μm, $n = 6$, $p = 4 \times 10^{-4}$; "Crush+BNN27 (2 drops/day)": 7.1 ± 0.4 cells/100 μm, $n = 8$, $p = 10^{-4}$]. Administration of two BNN27 drops per day did not enhance NeuN$^+$ cell density compared to one drop per day ($p > 0.99$) (Figure 1f). LC-MSn analysis in eye tissues harvested 24 h after the last drop administration (1 week post ONC) detected BNN27 in 1 out of 6 optic nerve samples and 1 out of 6 retina samples (in contralateral eyes BNN27 was detected in 2/6 optic nerve and 2/6 retina samples).

3.3 | CGS-FmocFF Grafts for Local BNN27 Delivery at ONC Sites

Due to the limitations of therapeutic molecule delivery in the retina via eye drops [40, 41], we implemented targeted MNT delivery in the ONC site via the encapsulation of BNN27 in a FmocFF peptide hydrogel [42] that was formed inside a CGS backbone (Figure 2a). Due to limitations imposed by BNN27 solubility and hydrogel peptide preparation, BNN27-loaded grafts contained 6 μL 30 mM BNN27 in 25% ethanol solution. BNN27-loaded CGS-FmocFF grafts were carefully placed around the ONC site immediately following injury ["Crush+BNN27 (Graft)" group] (Figure 2b,c). Once the graft was placed around the optic nerve, the encapsulated BNN27 diffused from the graft into surrounding tissues. In vitro release experiments of BNN27 from FmocFF hydrogel into 0.05% Tween20-PBS solution displayed first order kinetics with a time constant of $\tau = 17.9 \pm 4.8$ h (Figure 2e). To verify biomaterial graft placement, grafts that contained fluorescein isothiocynate (FITC)-labeled CGS were implanted at ONC sites. Ten days later, grafts were still observed at the original placement around the optic nerve (Figure 2f). LC-MSn revealed the presence of BNN27 2 weeks post graft implantation in 1 out of 5 optic nerve samples and in 2 out of 5 retina samples. BNN27 was not detected in the retina or optic nerve of contralateral eyes.

3.4 | Effects of BNN27 Delivered via CGS-FmocFF Grafts Following ONC

The effects of BNN27 administration via CGS-FmocFF grafts were compared to the effects of BNN27 administration via eye drops. The study included four groups described above: "Crush," "Crush (Graft)," "Crush+BNN27 (2 drops/day)," and "Crush+BNN27 (Graft)" groups. Quantification of the linear density of NeuN$^+$ cells in the GCL of peripheral retina showed a significant loss of RGCs in the GCL of injured eyes at 2 wpi ("Intact": 9.5 ± 0.7 cells/100 μm, $n = 5$; "Crush": 3.6 ± 0.3 cells/100 μm, $n = 7$, $p < 10^{-4}$). Graft placement lacking BNN27 resulted in increased RGC survival at 2 wpi compared to "Crush" group ["Crush": 3.6 ± 0.3 cells/100 μm, $n = 7$; "Crush (Graft)": 6.3 ± 0.5 cells/100 μm, $n = 4$, $p = 0.004$]. BNN27 delivered via both methods (eye drops or grafts) significantly increased RGC survival at 2 wpi compared to "Crush" group ["Crush": 3.6 ± 0.3 cells/100 μm, $n = 7$; "Crush+BNN27 (2 drops/day)": 7.1 ± 0.4 cells/100 μm, $n = 8$, $p < 10^{-4}$; "Crush+BNN27 (Graft)": 8.8 ± 0.2 cells/100 μm, $n = 9$, $p < 10^{-4}$]. Targeted administration of BNN27 via grafts resulted in higher and more consistent (less variation) RGC survival compared to administration via eye drops ["Crush+BNN27 (2 drops/day)" vs. "Crush+BNN27 (Graft)": $p = 0.02$] or graft placement lacking BNN27 ["Crush (Graft)" vs. "Crush+BNN27 (Graft)": $p = 0.004$], which was not statistically different from the one measured in intact eyes ["Intact" vs. "Crush+BNN27 (Graft)": $p = 0.71$] (Figure 3).

Significant axonal degeneration was observed in the optic nerve at 2 wpi. Double immunostaining of optic nerve sections using a pan-neurofilament (NF; neuronal marker) antibody and a MAG (myelin marker) antibody revealed significant loss of axon myelin integrity, since MAG, a known inhibitor of axon regeneration, was released from damaged myelin (Figure 4a). Immunostaining of optic nerve sections for the L1 cell adhesion molecule [upregulated in elongating axons [43]] highlighted the proximal end of the injury site, where a high accumulation of L1$^+$ RGC axons was observed (Figure 4b). Quantification of L1$^+$ axons at various distances away from the proximal end of the injury site showed no significant effect of BNN27 on axonal elongation at 2 wpi compared to the "Crush" group [750 μm away from the proximal end: "Crush" 6.8 ± 0.9 axons/100 μm, $n = 4$; "Crush (Graft)" 4.2 ± 0.7 axons/100 μm, $n = 4$, $p = 0.53$; "Crush+BNN27 (2 drops/day)" 7.6 ± 2.3 axons/100 μm, $n = 3$, $p = 0.97$; "Crush+BNN27 (Graft)" 5.6 ± 1.0 axons/100 μm, $n = 5$, $p = 0.88$] (Figure 4c). In all groups, L1$^+$ axons were almost absent after the injury site.

Finally, quantification of the fraction of Iba1$^+$ (microglia marker) pixels within the lesion (Figure 4d) showed that BNN27 administration decreased microglia density at the injury site at 2 wpi compared to "Crush" group. This decrease was significant only when BNN27 was delivered via grafts, whereas eye drops delivery showed high variability ["Crush": 26.7% ± 1.9%, $n = 4$; "Crush+BNN27 (2 drops/day)": 18.1% ± 5.2%, $n = 4$, $p = 0.2$; "Crush+BNN27 (Graft)": 14.6% ± 1.8%, $n = 5$, $p = 0.04$] (Figure 4e).

4 | Discussion

Due to their ability to imitate the actions of endogenous NTs, MNT-based treatments have been considered as potential therapeutics for several neurological disorders [18], showing promising results in various rodent models, including diabetic-induced retinal damage [23] and SCI [26]. Here, we provide the first report on the therapeutic effects of BNN27, a small-molecule mimicking NGF actions, in an animal model of ONI.

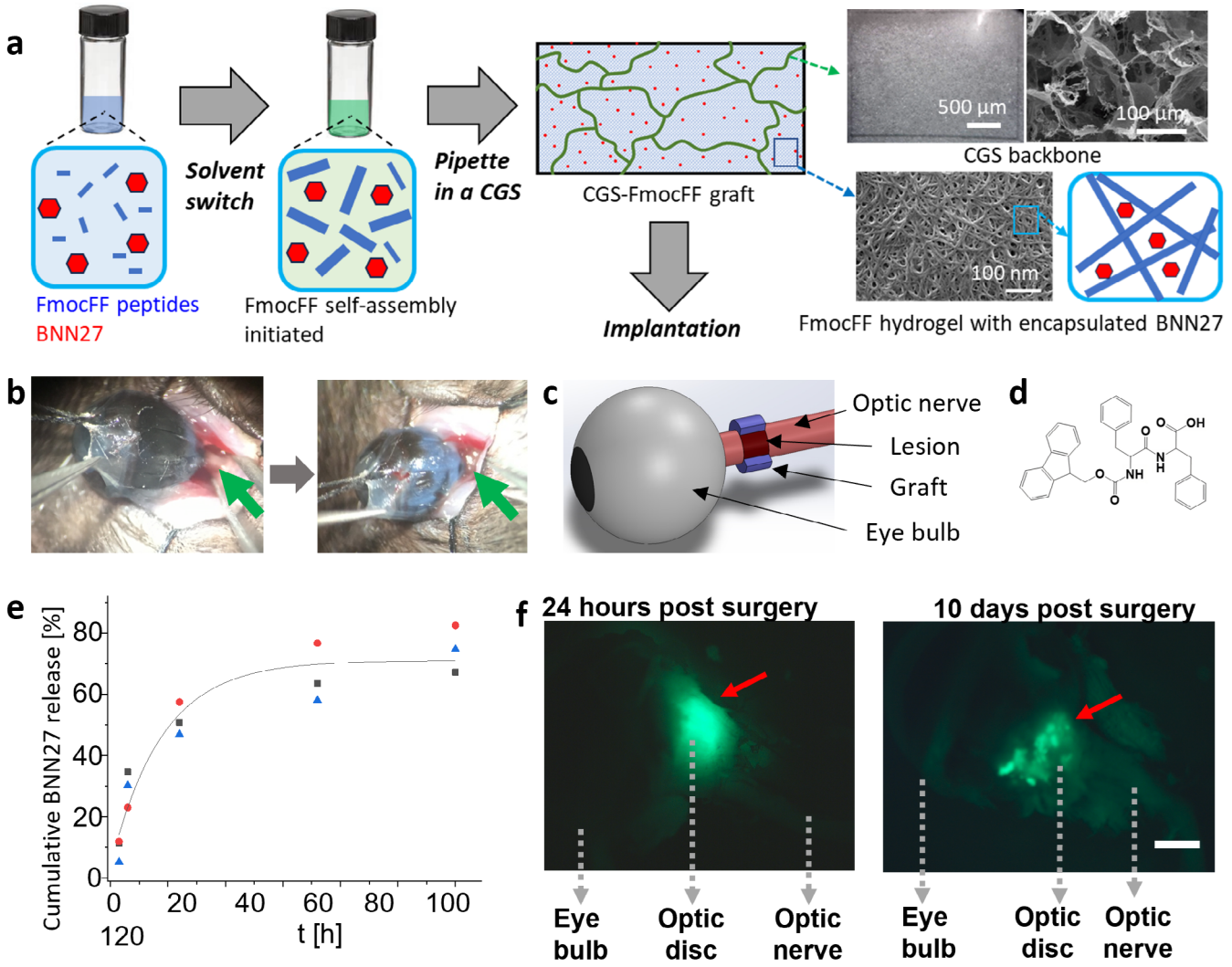

FIGURE 2 | Fabrication, characterization, and implantation of CGS-FmocFF grafts for localized delivery of BNN27 in ONC sites. (a) BNN27-loaded CGS-FmocFF grafts consist of a CGS backbone (imaged via optical microscopy (left) and SEM (right)) that houses an FmocFF hydrogel (imaged via SEM) that encapsulates BNN27. (b) Implantation of BNN27-loaded CGS-FmocFF graft around the surgically exposed optic nerve. Green arrows indicate the optic nerve before the implantation (left) and the graft placed around the optic nerve (right). (c) Schematic representation of a BNN27-loaded CGS-FmocFF graft placed around the optic nerve in the ONC site. (d) Structure of FmocFF peptides. (e) Kinetics of BNN27 release $n(t)/n_0$ from a FmocFF hydrogel into a 0.05% Tween20-PBS solution. (f) Fluorescence imaging of FITC-labeled CGS grafts (red arrows) reveals their presence around the optic nerve 24 h and 10 days post-surgery. Scale bar: 1 mm.

In agreement with previous studies [44], we show that both NGF receptors ($p75^{NTR}$, TrkA) are expressed in GCL cells (Figure 1), suggesting that they can respond to BNN27. Our results do not provide conclusions on ONI effects on NTR expression. Published reports on ONI-induced NTR expression alterations are contradictory, depending on the time and method of quantification [45]. We show that ONC induced a trend of $p75^{NTR}$ upregulation and TrkA downregulation at 2 wpi (Figure 1), which agrees with the proposed deregulation of NGF receptor signaling balance in favor of proNGF/$p75^{NTR}$ signaling [45], yet observed differences were not statistically significant.

We utilized the mouse ONC model, which has been used to study key ONI events including RGC death and axonal elongation [46]. Our results indicated that 60%–70% of $NeuN^+$ RGCs were lost at 2 wpi following ONC (Figures 1 and 3), replicating previous reports [47]. Differences in RGC survival reported in the literature could arise from the elegant nature of the ONC operation, as different users could induce crush of variable severity. Our consistent results on RGC survival following ONC highlight the accuracy and reproducibility of our manipulations.

BNN27 was delivered via eye drops or via CGS-FmocFF grafts placed around the injured optic nerve. BNN27 administration increased RGC survival compared to non-treated injured eyes at 2 wpi (Figures 1 and 3), in agreement with previous reports on the ability of NGF to reduce RGC loss in vivo [13, 14]. The low bioavailability of eye drops for retinal drug delivery (< 3% of administered therapeutics reach the retina [41, 48]) could explain why daily administration of BNN27 drops was required for neuroprotective effects, while administration every second day did not affect RGC survival at 2 wpi (Figure 1).

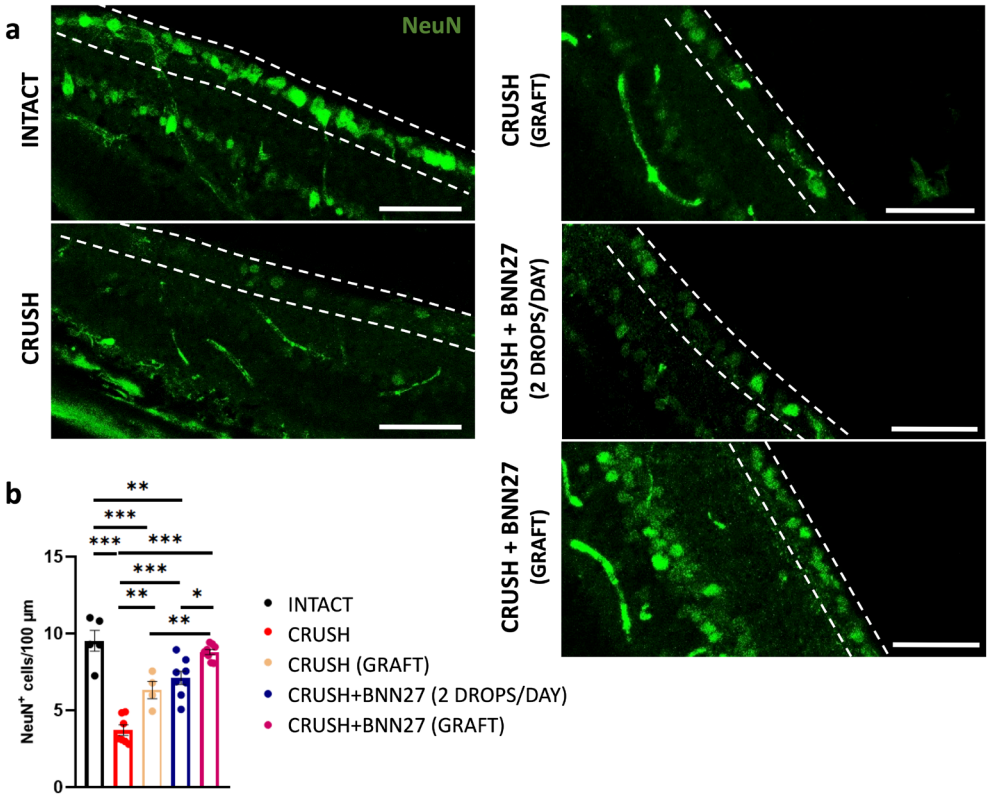

FIGURE 3 | Evaluation of BNN27 effects on RGC survival at 2 wpi when delivered via CGS-FmocFF grafts. (a) Representative fluorescence images of peripheral retina cross sections from all groups immunostained for NeuN. GCL boundaries are denoted by dotted lines. Scale bars: 50 μm. (b) Quantification of NeuN$^+$ cell linear density in the GCL of peripheral retina at 2 wpi ["Intact": $N = 5$; "Crush": $N = 7$; "Crush (Graft)": $N = 4$; "Crush+BNN27 (2 drops/day)": $N = 8$; "Crush+BNN27 (Graft)": $N = 9$]. Results are presented as mean ± SEM. $^*p < 0.05$, $^{**}p < 0.01$, $^{***}p < 0.001$; Tukey's post hoc pairwise test assuming $p_{1\text{-way-ANOVA}} < 0.05$.

Axonal degeneration begins soon after ONC and is associated with cytoskeleton alterations and autophagy linked to increased intra-axonal Ca^{2+} levels [49]. Here, ONC resulted in extensive axonal degeneration and loss of axon myelin integrity at 2 wpi. Released MAG from damaged myelin (Figure 4) is a key inhibitor of axon regeneration. Spontaneous RGC axon regeneration was limited, as just 0.2% of axons were reported to reach the optic chiasm 1 month post-injury [47]. Since axonal dysfunction precedes RGC death, promoting axon regeneration to strengthen axonal transport of molecules and organelles is crucial for RGC survival [50]. However, in our study, BNN27 failed to prevent axonal degeneration or promote regeneration at 2 wpi (Figure 4), in agreement with the reported inability of BNN27 alone to promote neurite extension [21].

Following ONI, inflammation initiates within minutes and involves many cell types, including microglia. Despite some beneficial effects, inflammation leads to further tissue damage and neuronal death. Inhibition of microglial activation after ONI promoted RGC survival [51]. BNN27 administration via grafts significantly decreased ONC-induced microglia-mediated inflammation at the injury site at 2 wpi compared to untreated eyes (Figure 4), in agreement with the reported activation of anti-inflammatory TrkA-mediated pathways (PI3K-Akt1/Akt2-CREB) by NGF and DHEA [52, 53], and the reported anti-inflammatory effects (reduced secretion of pro-inflammatory cytokines, increased secretion of anti-inflammatory cytokines) of BNN27 administration in a rat model of diabetic-induced retinal damage [23].

This study also presents the first case of MNT administration in vivo via a biomaterial graft. Delivery of small-molecule compounds via biomaterial grafts can target therapeutics at injury sites and reduce side effects to other tissues [37]. Here, BNN27 was encapsulated in a FmocFF peptide hydrogel formed inside a CGS. Once the hydrogel formed, the resulting BNN27-loaded CGS-FmocFF graft was placed around the injured optic nerve to deliver BNN27 near the lesion (Figure 2). The CGS backbone of the graft provided mechanical support, housed the FmocFF hydrogel, and prevented foreign body response, as has been demonstrated in established applications of CGS in regenerative medicine [54]. Hydrogels consisting of the ionic self-complementary 16-amino acid peptide RADA16-1 were first used by Zhang and colleagues to support optic nerve regeneration [55]. Due to the aromatic nature of the FmocFF peptide, FmocFF hydrogels are appropriate for the encapsulation of hydrophobic compounds such as BNN27. Moreover, the piezoelectric properties of self-assembled FmocFF peptides have been associated with axonal regeneration and neuroprotection [42]. In this study, although placement of CGS-FmocFF graft lacking BNN27 around the injured optic nerve could not promote axonal elongation, yet it enhanced RGC survival at 2 wpi (Figure 3) compared to the "Crush" group. BNN27 release from FmocFF hydrogels into aqueous solution followed first order kinetics with a $\tau = 17.9$ h time constant (Figure 2). Assuming that in vivo kinetics have similar

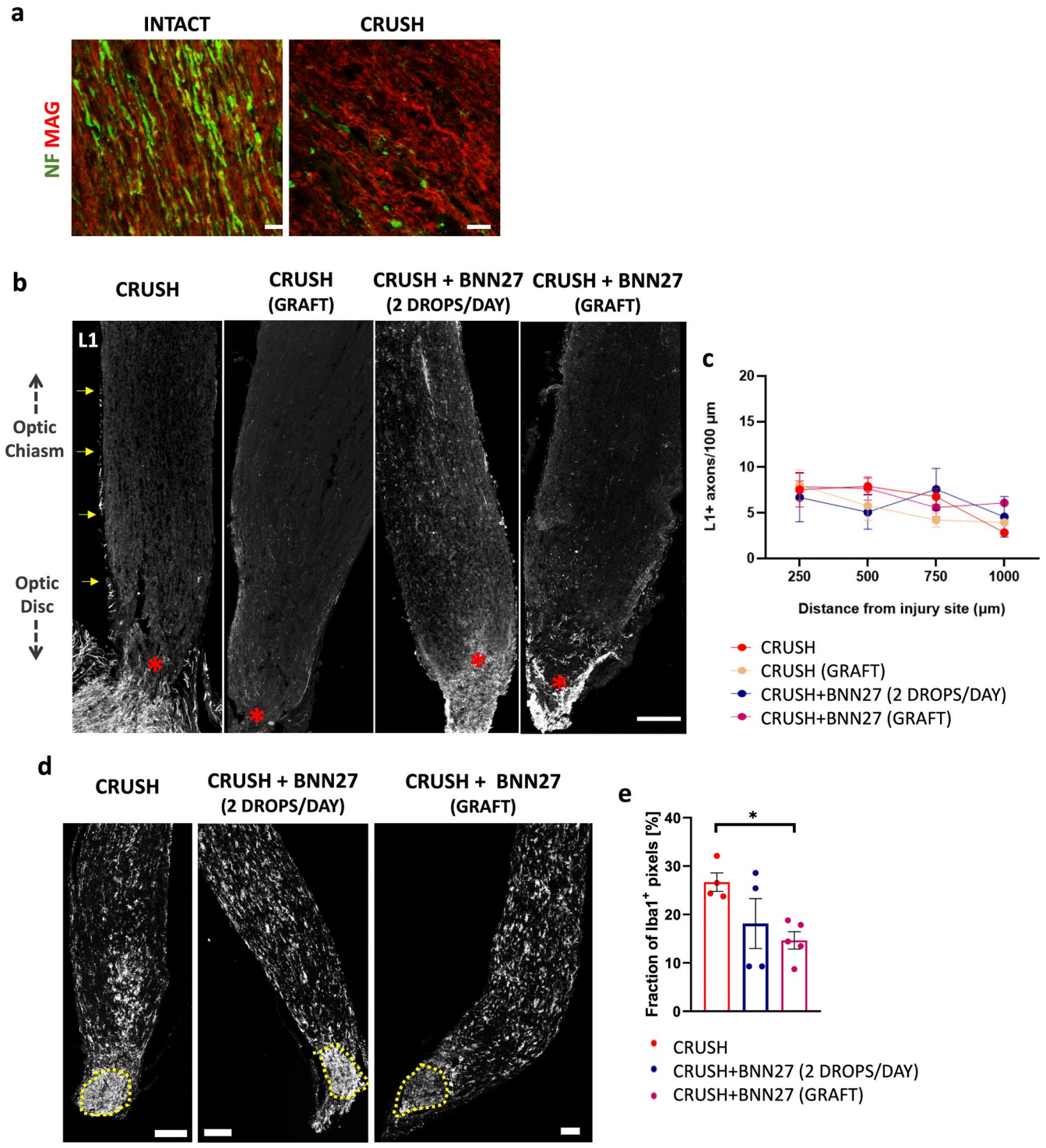

FIGURE 4 | BNN27 effects on axonal elongation in the optic nerve and on microglia-mediated inflammation in the ONC site at 2 wpi. (a) Representative fluorescence images of optic nerve longitudinal sections from intact and injured eyes at 2 wpi immunostained for NF (green) and MAG (red) markers. Scale bars: 10 μm. (b) Representative fluorescence images of longitudinal sections of crushed optic nerves immunostained for L1. The proximal end of the injury site is noted with a red asterisk. Yellow arrows point to specific distances (250, 500, 750, and 1000 μm) away from the proximal end of the ONC site. Scale bar: 100 μm. (c) Quantification of the linear density of $L1^+$ axons per section at 250, 500, 750, and 1000 μm away from the proximal end of the ONC site at 2 wpi ["Crush": $N = 4$; "Crush (Graft)": $N = 4$; "Crush+BNN27 (2 drops/day)": $N = 3$; "Crush+BNN27 (Graft)": $N = 5$]. (d) Representative fluorescence images of longitudinal sections of crushed optic nerves immunostained for Iba1. The ONC site is defined by a dotted line. Scale bars: 100 μm. (e) Quantification of the fraction of $Iba1^+$ pixels within the ONC site at 2 wpi ["Crush": $N = 4$; "Crush+BNN27 (2 drops/day)": $N = 4$; "Crush+BNN27 (Graft)": $N = 5$]. Results are presented as mean ± SEM. *$p < 0.05$; Tukey's post hoc pairwise test assuming $p_{\text{1-way-ANOVA}} < 0.05$.

kinetics, our data suggest that BNN27 release over a period of at least $4\tau \approx 4$ days was enough to induce significant neuroprotective effects on RGC at 2 wpi (Figure 3). Indeed, we verified that 10 days following implantation, the CGS graft backbone was still located around the injured optic nerve (Figure 2) and that 14 days following graft implantation BNN27 was detected in eye tissues. In summary, casting FmocFF hydrogels within CGS establishes a "biomaterial-within-biomaterial" strategy that combines structural support and sustained release of BNN27.

A key finding of this study is that BNN27 delivery via biomaterial grafts placed around an ONC lesion offers advantages compared to the established delivery method via eye drops. Specifically, BNN27 delivery via CGS-FmocFF grafts resulted in enhanced and more consistent RGC neuroprotection at 2 wpi (Figure 3). This neuroprotective effect was also significantly greater than that observed with CGS-FmocFF grafts lacking BNN27, highlighting the importance of the combinatorial treatment. Furthermore, BNN27 effects on microglia-mediated inflammation in the ONC lesion were statistically significant only when BNN27 was delivered via CGS-FmocFF grafts (Figure 4). While previous studies have shown that local delivery of therapeutics in an ONI lesion via biomaterial grafts can enhance RGC survival [56], our study directly compares the effects of therapeutic delivery via eye drops or via a biomaterial graft placed around the optic nerve.

5 | Conclusion

BNN27 administration in the mouse ONC model significantly enhanced RGC survival in the lesion site at 2 weeks following injury. Compared to standard delivery via eye drops, local delivery of BNN27 in the optic nerve via CGS-FmocFF grafts resulted in increased and more consistent RGC neuroprotection as well as decreased microglia-mediated inflammation. RGC survival is a necessary yet insufficient condition for vision restoration following ONI, as enhanced RGC survival does not always lead to enhanced axonal regeneration [57]. Indeed, we showed that BNN27 administration did not affect RGC axon regeneration. Yet, we propose that the neuroprotective effects of BNN27-loaded CGS-FmocFF grafts can form the basis of novel treatments for ONI, where BNN27 effects will be complemented by therapeutic molecules that can enhance and guide the elongation of surviving axons toward their targets.

Author Contributions

Conceptualization: K.G., A.M., I.C., A.G., D.S.T. Data curation: K.G., D.S.T. Funding acquisition: K.G., K.K., M.S., D.S.T. Investigation: K.G., E.A.S., C.P.A., X.M., A.P. Methodology: K.G., C.P.A., T.K., T.C., K.K., A.M., I.C., A.G., M.S., D.S.T. Project administration: K.G., K.K., I.C., A.G., D.S.T. Resources: A.M., T.K., T.C., D.K., I.C., A.G., M.S., D.S.T. Supervision: I.C., A.G., M.S., D.S.T. Validation: K.G., D.S.T. Visualization: K.G., D.S.T. Writing – original draft: K.G., D.S.T. Writing – review and editing: all.

Acknowledgments

We thank F. Moschogiannaki for assistance in CGS fabrication and for providing the images of Figure 2a, and Professor F. Rathjen (Max-Delbrück-Centrum für Molekulare Medizin, Germany) for providing the L1 antibody. The publication of this article in OA mode was financially supported by HEAL-Link.

This research was funded by the Hellenic Foundation for Research and Innovation (HFRI) and the General Secretariat for Research and Technology (GSRT) under grant agreement no. 1635 to D.S.T., M.S., and K.K., and by a Greek State Scholarships Foundation (IKY) scholarship to K.G.

Funding

This work was supported by Hellenic Foundation for Research and Innovation (HFRI) and the General Secretariat for Research and Technology (GSRT) (Grant No. 1635).

Conflicts of Interest

Dr. A. Gravanis is the co-founder of spin-off Bionature E.A. Ltd (www.bionature.net), proprietary of compound BNN27 (Patent WO2008/155534 A2). The remaining authors declare no conflicts of interest.

Data Availability Statement

The data that support the findings of this study are available from the corresponding author upon reasonable request.

References

1. N. Sarkies, "Traumatic Optic Neuropathy," *Eye* 18 (2004): 1122–1125, https://doi.org/10.1038/sj.eye.6701571.

2. L. Sun, Y. Cen, X. Liu, et al., "Systemic Whole Transcriptome Analysis Identified Underlying Molecular Characteristics and Regulatory Networks Implicated in the Retina Following Optic Nerve Injury," *Experimental Eye Research* 244 (2024): 109929, https://doi.org/10.1016/j.exer.2024.109929.

3. P. Yu-Wai-Man, "Traumatic Optic Neuropathy—Clinical Features and Management Issues," *Taiwan Journal of Ophthalmology* 5 (2015): 3–8, https://doi.org/10.1016/j.tjo.2015.01.003.

4. S. de Lima, Y. Koriyama, T. Kurimoto, et al., "Full-Length Axon Regeneration in the Adult Mouse Optic Nerve and Partial Recovery of Simple Visual Behaviors," *Proceedings of the National Academy of Sciences of the United States of America* 109, no. 23 (2012): 9149–9154, https://doi.org/10.1073/pnas.1119449109.

5. J. J. Scott-McKean, M. Matsuyama, C. W. Guo, et al., "Cytoprotective Small Compound M109S Attenuated Retinal Ganglion Cell Degeneration Induced by Optic Nerve Crush in Mice," *Cells* 13, no. 11 (2024): 911, https://doi.org/10.3390/cells13110911.

6. V. da Barros Ribeiro Silva, M. Porcionatto, and V. Toledo Ribas, "The Rise of Molecules Able to Regenerate the Central Nervous System," *Journal of Medicinal Chemistry* 63, no. 2 (2020): 490–511, https://doi.org/10.1021/acs.jmedchem.9b00863.

7. B. Laha, B. K. Stafford, and A. D. Huberman, "Regenerating Optic Pathways From the Eye to the Brain," *Science* 356, no. 6342 (2017): 1031–1034, https://doi.org/10.1126/science.aal5060.

8. M. V. Chao, "Neurotrophins and Their Receptors: A Convergence Point for Many Signalling Pathways," *Nature Reviews. Neuroscience* 4 (2003): 299–309, https://doi.org/10.1038/nrn1078.

9. L. F. Reichardt, "Neurotrophin-Regulated Signalling Pathways," *Philosophical Transactions of the Royal Society, B: Biological Sciences* 361 (2006): 1545–1564, https://doi.org/10.1098/rstb.2006.1894.

10. N. Yamashita, "Retrograde Signaling via Axonal Transport Through Signaling Endosomes," *Journal of Pharmacological Sciences* 141, no. 2 (2019): 91–96, https://doi.org/10.1016/j.jphs.2019.10.001.

11. E. C. Johnson, Y. Guo, W. O. Cepurna, and J. C. Morrison, "Neurotrophin Roles in Retinal Ganglion Cell Survival: Lessons From Rat

Glaucoma Models," *Experimental Eye Research* 88 (2009): 808–815, https://doi.org/10.1016/j.exer.2009.02.004.

12. P. Candeo, G. Carmignoto, L. Maffei, R. Canella, and C. Comelli, "NGF Effects on the Survival of Rat Retinal Ganglion Cells Following Optic Nerve Section," *Pharmacological Research Communications* 20 (1988): 65, https://doi.org/10.1016/S0031-6989(88)80195-4.

13. L. Guo, B. M. Davis, N. Ravindran, et al., "Topical Recombinant Human Nerve Growth Factor (rh-NGF) is Neuroprotective to Retinal Ganglion Cells by Targeting Secondary Degeneration," *Scientific Reports* 10 (2020): 1–13, https://doi.org/10.1038/s41598-020-60427-2.

14. L. A. Mesentier-Louro, P. Rosso, V. Carito, et al., "Nerve Growth Factor Role on Retinal Ganglion Cell Survival and Axon Regrowth: Effects of Ocular Administration in Experimental Model of Optic Nerve Injury," *Molecular Neurobiology* 56 (2019): 1056–1069, https://doi.org/10.1007/s12035-018-1154-1.

15. S. Josephy-Hernandez, S. Jmaeff, I. Pirvulescu, T. Aboulkassim, and H. U. Saragovi, "Neurotrophin Receptor Agonists and Antagonists as Therapeutic Agents: An Evolving Paradigm," *Neurobiology of Disease* 97 (2017): 139–155, https://doi.org/10.1016/j.nbd.2016.08.004.

16. K. M. Keefe, I. S. Sheikh, and G. M. Smith, "Targeting Neurotrophins to Specific Populations of Neurons: NGF, BDNF, and NT-3 and Their Relevance for Treatment of Spinal Cord Injury," *International Journal of Molecular Sciences* 18 (2017): 1–17, https://doi.org/10.3390/ijms18030548.

17. T. Calogeropoulou, N. Avlonitis, N. Minas, et al., "Novel Dehydroepiandrosterone Derivatives With Antiapoptotic, Neuroprotective Activity," *Journal of Medicinal Chemistry* 52, no. 21 (2009): 6569–6587, https://doi.org/10.1021/jm900468p.

18. A. Gravanis, I. Pediaditakis, and I. Charalampopoulos, "Synthetic Microneurotrophins in Therapeutics of Neurodegeneration," *Oncotarget* 8 (2017): 9005–9006, https://doi.org/10.18632/oncotarget.14667.

19. J. P. Bennett, L. C. O'Brien, and D. G. Brohawn, "Pharmacological Properties of Microneurotrophin Drugs Developed for Treatment of Amyotrophic Lateral Sclerosis," *Biochemical Pharmacology* 117 (2016): 68–77, https://doi.org/10.1016/j.bcp.2016.08.001.

20. C. Tsika, M. N. Tzatzarakis, S. G. Antimisiaris, et al., "Quantification of BNN27, a Novel Neuroprotective 17-Spiroepoxy Dehydroepiandrosterone Derivative in the Blood and Retina of Rodents, After Single Intraperitoneal Administration," *Pharmacology Research & Perspectives* 9 (2021): 1–8, https://doi.org/10.1002/prp2.724.

21. I. Pediaditakis, P. Efstathopoulos, K. C. Prousis, et al., "Selective and Differential Interactions of BNN27, a Novel C17-Spiroepoxy Steroid Derivative, With TrkA Receptors, Regulating Neuronal Survival and Differentiation," *Neuropharmacology* 111 (2016): 266–282, https://doi.org/10.1016/j.neuropharm.2016.09.007.

22. I. Pediaditakis, A. Kourgiantaki, K. C. Prousis, et al., "BNN27, a 17-Spiroepoxy Steroid Derivative, Interacts With and Activates p75 Neurotrophin Receptor, Rescuing Cerebellar Granule Neurons From Apoptosis," *Frontiers in Pharmacology* 7 (2016): 512, https://doi.org/10.3389/fphar.2016.00512.

23. R. Ibán-Arias, S. Lisa, N. Mastrodimou, et al., "The Synthetic Microneurotrophin BNN27 Affects Retinal Function in Rats With Streptozotocin-Induced Diabetes," *Diabetes* 67 (2018): 321–333, https://doi.org/10.2337/db17-0391.

24. R. Ibán-Arias, S. Lisa, S. Poulaki, et al., "Effect of Topical Administration of the Microneurotrophin BNN27 in the Diabetic Rat Retina," *Graefe's Archive for Clinical and Experimental Ophthalmology* 257 (2019): 2429–2436, https://doi.org/10.1007/s00417-019-04460-6.

25. G. Bonetto, I. Charalampopoulos, A. Gravanis, and D. Karagogeos, "The Novel Synthetic Microneurotrophin BNN27 Protects Mature Oligodendrocytes Against Cuprizone-Induced Death, Through the NGF Receptor TrkA," *Glia* 65 (2017): 1376–1394, https://doi.org/10.1002/glia.23170.

26. K. Georgelou, E. A. Saridaki, K. Karali, et al., "Microneurotrophin BNN27 Reduces Astrogliosis and Increases Density of Neurons and Implanted Neural Stem Cell-Derived Cells After Spinal Cord Injury," *Biomedicine* 11 (2023): 1170, https://doi.org/10.3390/biomedicines11041170.

27. A. Mahler, M. Reches, M. Rechter, S. Cohen, and E. Gazit, "Rigid, Self-Assembled Hydrogel Composed of a Modified Aromatic Dipeptide," *Advanced Materials* 18 (2006): 1365–1370, https://doi.org/10.1002/adma.200501765.

28. G. Fichman and E. Gazit, "Self-Assembly of Short Peptides to Form Hydrogels: Design of Building Blocks, Physical Properties and Technological Applications," *Acta Biomaterialia* 10, no. 4 (2014): 1671–1682, https://doi.org/10.1016/j.actbio.2013.08.013.

29. C. Diaferia, G. Morelli, and A. Accardo, "Fmoc-Diphenylalanine as a Suitable Building Block for the Preparation of Hybrid Materials and Their Potential Applications," *Journal of Materials Chemistry B* 7 (2019): 5142–5155, https://doi.org/10.1039/C9TB01043B.

30. R. Choe and S. I. Yun, "Fmoc-Diphenylalanine-Based Hydrogels as a Potential Carrier for Drug Delivery," *E-Polymers* 20 (2020): 458–468, https://doi.org/10.1515/epoly-2020-0050.

31. C. P. Apostolidou, C. Kokotidou, V. Platania, et al., "Antimicrobial Potency of Fmoc-Phe-Phe Dipeptide Hydrogels With Encapsulated Porphyrin Chromophores is a Promising Alternative in Antimicrobial Resistance," *Biomolecules* 14, no. 2 (2024): 226, https://doi.org/10.3390/biom14020226.

32. I. A. Dontas, P. Lelovas, S. Parara, et al., "Delivery of Porphyrins Through Self-Assembling Peptide Hydrogels for Accelerated Healing of Experimental Skin Defects in Vivo," *Cureus* 15, no. 5 (2023): e39120, https://doi.org/10.7759/cureus.39120.

33. E. Gallo, C. Diaferia, E. Rosa, G. Smaldone, G. Morelli, and A. Accardo, "Peptide-Based Hydrogels and Nanogels for Delivery of Doxorubicin," *International Journal of Nanomedicine* 16 (2021): 1617–1630, https://doi.org/10.2147/IJN.S296272.

34. E. Gallo, C. Diaferia, G. Smaldone, et al., "Fmoc-FF Hydrogels and Nanogels for Improved and Selective Delivery of Dexamethasone in Leukemic Cells and Diagnostic Applications," *Scientific Reports* 14 (2024): 9940, https://doi.org/10.1038/s41598-024-60145-z.

35. P. Divanach, A. Noti, P. Vouvopoulos, et al., "FmocFF Peptide Hydrogel is a Promising Matrix for Encapsulation and Controlled Release of the Anticancer Peptide Drug Bortezomib," *Biomolecules* 15 (2025): 839, https://doi.org/10.3390/biom15060839.

36. F. O'Brien, B. A. Harley, I. V. Yannas, and L. Gibson, "Influence of Freezing Rate on Pore Structure in Freeze-Dried Collagen-GAG Scaffolds," *Biomaterials* 25 (2004): 1077–1086, https://doi.org/10.1016/s0142-9612(03)00630-6.

37. S. Tehrani, R. K. Delf, W. O. Cepurna, L. Davis, E. C. Johnson, and J. C. Morrison, "In Vivo Small Molecule Delivery to the Optic Nerve in a Rodent Model," *Scientific Reports* 8 (2018): 1–9, https://doi.org/10.1038/s41598-018-22737-4.

38. Z. Tang, S. Zhang, C. Lee, et al., "An Optic Nerve Crush Injury Murine Model to Study Retinal Ganglion Cell Survival," *Journal of Visualized Experiments* 50 (2011): e2685, https://doi.org/10.3791/2685.

39. M. Kannavou, K. Karali, T. Katsila, et al., "Development and Comparative In Vitro and In Vivo Study of BNN27 Mucoadhesive Liposomes and Nanoemulsions for Nose-to-Brain Delivery," *Pharmaceutics* 15, no. 2 (2023): 419, https://doi.org/10.3390/pharmaceutics15020419.

40. K. Nayak and M. Misra, "A Review on Recent Drug Delivery Systems for Posterior Segment of Eye," *Biomedicine & Pharmacotherapy* 107 (2018): 1564–1582, https://doi.org/10.1016/j.biopha.2018.08.138.

41. A. Subrizi, E. M. del Amo, V. Korzhikov-Vlakh, T. Tennikova, M. Ruponen, and A. Urtti, "Design Principles of Ocular Drug Delivery

Systems: Importance of Drug Payload, Release Rate, and Material Properties," *Drug Discovery Today* 24 (2019): 1446–1457, https://doi.org/10.1016/j.drudis.2019.02.001.

42. K. Ryan, J. Beirne, G. Redmond, et al., "Nanoscale Piezoelectric Properties of Self-Assembled Fmoc-FF Peptide Fibrous Networks," *ACS Applied Materials & Interfaces* 7 (2015): 12702–12707, https://doi.org/10.1021/acsami.5b01251.

43. M. Savvaki, G. Kafetzis, S. I. Kaplanis, N. Ktena, K. Theodorakis, and D. Karagogeos, "Neuronal, but Not Glial, Contactin 2 Negatively Regulates Axon Regeneration in the Injured Adult Optic Nerve," *European Journal of Neuroscience* 53 (2021): 1705–1721, https://doi.org/10.1111/ejn.15121.

44. N. Parmhans, S. Sajgo, J. Niu, W. Luo, and T. C. Badea, "Characterization of Retinal Ganglion Cell, Horizontal Cell, and Amacrine Cell Types Expressing the Neurotrophic Receptor Tyrosine Kinase Ret," *Journal of Comparative Neurology* 526, no. 4 (2018): 742–766, https://doi.org/10.1002/cne.24367.

45. T. B. Garcia, M. Hollborn, and A. Bringmann, "Expression and Signaling of NGF in the Healthy and Injured Retina," *Cytokine & Growth Factor Reviews* 34 (2017): 43–57, https://doi.org/10.1016/j.cytogfr.2016.11.005.

46. G. G. Bastakis, N. Ktena, D. Karagogeos, and M. Savvaki, "Models and Treatments for Traumatic Optic Neuropathy and Demyelinating Optic Neuritis," *Developmental Neurobiology* 79 (2019): 819–836, https://doi.org/10.1002/dneu.22710.

47. H.-J. Li, Z.-L. Sun, X.-T. Yang, L. Zhu, and D.-F. Feng, "Exploring Optic Nerve Axon Regeneration," *Current Neuropharmacology* 15 (2017): 861–873, https://doi.org/10.2174/1570159X14666161227150250.

48. G. A. Rodrigues, D. Lutz, J. Shen, et al., "Topical Drug Delivery to the Posterior Segment of the Eye: Addressing the Challenge of Preclinical to Clinical Translation," *Pharmaceutical Research* 35, no. 12 (2018): 245, https://doi.org/10.1007/s11095-018-2519-x.

49. J. Knöferle, J. C. Koch, T. Ostendorf, et al., "Mechanisms of Acute Axonal Degeneration in the Optic Nerve in Vivo," *Proceedings of the National Academy of Sciences of the United States of America* 107 (2010): 6064–6069, https://doi.org/10.1073/pnas.0909794107.

50. L. I. Benowitz, Z. He, and J. L. Goldberg, "Reaching the Brain: Advances in Optic Nerve Regeneration," *Experimental Neurology* 287 (2017): 365–373, https://doi.org/10.1016/j.expneurol.2015.12.015.

51. H. Yu, B. Shen, R. Han, et al., "CX3CL1-CX3CR1 Axis Protects Retinal Ganglion Cells by Inhibiting Microglia Activation in a Distal Optic Nerve Trauma Model," *Inflammation and Regeneration* 44, no. 1 (2024): 30, https://doi.org/10.1186/s41232-024-00343-4.

52. V. I. Alexaki, G. Fodelianaki, A. Neuwirth, et al., "DHEA Inhibits Acute Microglia-Mediated Inflammation Through Activation of the TrkA-Akt1/2-CREB-Jmjd3 Pathway," *Molecular Psychiatry* 23 (2018): 1410–1420, https://doi.org/10.1038/mp.2017.167.

53. G. Minnone, F. De Benedetti, and L. Bracci-Laudiero, "NGF and Its Receptors in the Regulation of Inflammatory Response," *International Journal of Molecular Sciences* 18 (2017): 1028, https://doi.org/10.3390/ijms18051028.

54. I. V. Yannas, J. F. Burke, D. P. Orgill, and E. M. Skrabut, "Wound Tissue Can Utilize a Polymeric Template to Synthesize a Functional Extension of Skin," *Science* 215, no. 4529 (1982): 174–176, https://doi.org/10.1126/science.7031899.

55. R. G. Ellis-Behnke, Y. X. Liang, S. W. You, et al., "Nano Neuro Knitting: Peptide Nanofiber Scaffold for Brain Repair and Axon Regeneration With Functional Return of Vision," *Proceedings of the National Academy of Sciences of the United States of America* 103 (2006): 5054–5059, https://doi.org/10.1073/pnas.0600559103.

56. L. Li, F. Deng, H. Qiu, et al., "An Adherent Drug Depot for Retinal Ganglion Cell Protection and Regeneration in Rat Traumatic Optic Neuropathy Models," *RSC Advances* 11 (2021): 22761–22772, https://doi.org/10.1039/d0ra10362d.

57. B. Zheng and M. H. Tuszynski, "Regulation of Axonal Regeneration After Mammalian Spinal Cord Injury," *Nature Reviews. Molecular Cell Biology* 24, no. 6 (2023): 396–413, https://doi.org/10.1038/s41580-022-00562-y.